

Novel Mutations in the *RAD3* and *SSL1* Genes Perturb Genome Stability by Stimulating Recombination Between Short Repeats in *Saccharomyces cerevisiae*

Silvina Maines, M. Cristina Negritto, Xuli Wu, Glenn M. Manthey and Adam M. Bailis

Department of Molecular Biology, Beckman Research Institute, City of Hope National Medical Center, Duarte, California 91010

Manuscript received April 19, 1998

Accepted for publication June 24, 1998

ABSTRACT

Maintaining genome stability requires that recombination between repetitive sequences be avoided. Because short, repetitive sequences are the most abundant, recombination between sequences that are below a certain length are selectively restricted. Novel alleles of the *RAD3* and *SSL1* genes, which code for components of a basal transcription and UV-damage-repair complex in *Saccharomyces cerevisiae*, have been found to stimulate recombination between short, repeated sequences. In double mutants, these effects are suppressed, indicating that the *RAD3* and *SSL1* gene products work together in influencing genome stability. Genetic analysis indicates that this function is independent of UV-damage repair and mutation avoidance, supporting the notion that *RAD3* and *SSL1* together play a novel role in the maintenance of genome integrity.

IN the yeast *Saccharomyces cerevisiae*, homologous recombination is an important mechanism for repairing DNA damage (Friedberg *et al.* 1991). However, recombination between dispersed, repetitive sequences can result in deleterious genome rearrangements, such as deletions, insertions, inversions, and translocations (Petes and Hill 1988). One way to control these rearrangements is to restrict recombination to only the most similar sequences, thus blocking recombination between dispersed, duplicate sequences that have diverged over time (Shen and Huang 1986; Waldman and Liskay 1988; Bailis and Rothstein 1990; Bailis *et al.* 1992). This mechanism is under the control of certain mismatch repair genes in yeast (Selva *et al.* 1995; Datta *et al.* 1996; Negritto *et al.* 1997), *E. coli* (Feinstein and Low 1986; Radman 1988; Rayssiguier *et al.* 1989; Petit *et al.* 1991), and mammals (deWind *et al.* 1995).

Another way to reduce the frequency of genome rearrangement is to selectively restrict recombination between short repeats, because they are the most abundant (Britten and Kohne 1968). In yeast and mammalian cells, repeats below 250–300 bp recombine less well per unit length than longer sequences (Jinks-Robertson *et al.* 1993; Rubnitz and Subramani 1984). In yeast, sequences that share less than 30 bp are unable to interact by homologous recombination (Manivaskam *et al.* 1995). Rothstein and colleagues reported that in *S. cerevisiae*, deletions by recombination between δ elements,

a class of short repeats, is selectively stimulated by mutations in the *TOP3* gene (Wallis *et al.* 1989). Recently, we showed that a novel mutation in the *RAD3* gene also disrupts the control of short-repeat recombination (SRR) in *S. cerevisiae* (Bailis *et al.* 1995). Together, these observations suggest that there is a genetic basis for the selective discrimination against recombination between short repeats in yeast. Recent work suggests that a barrier against SRR could be important in humans, as homologous recombination between short repeats may give rise to tumor suppressor gene mutations in several cancers (Gu *et al.* 1994; Schichman *et al.* 1994; So *et al.* 1997).

The *S. cerevisiae* *RAD3* gene codes for a DNA-DNA and DNA-RNA helicase (Sung *et al.* 1987) that is a component of a heteropentameric complex at the core of both the transcription initiation factor TFIIF and the nucleotide excision repair (NER) complex (Feaver *et al.* 1993; Wang *et al.* 1994). The components of the heteropentamer are structurally and functionally conserved from yeast to humans (Gerard *et al.* 1991; Fischer *et al.* 1992; Hoelijmakers 1993; Humbert *et al.* 1994; Schaeffer *et al.* 1994). Many *rad3* mutations that confer a broad array of phenotypes have been identified: temperature-sensitive growth (Naumovski and Friedberg 1986; Guzder *et al.* 1994; Bailis *et al.* 1995); defective transcription (Guzder *et al.* 1994); UV sensitivity (Reynolds and Friedberg 1981; Wilcox and Prakash 1981; Song *et al.* 1990); elevated mutation rate (Montelone *et al.* 1988; Song *et al.* 1990); and elevated frequencies of spontaneous recombination (Montelone *et al.* 1988; Song *et al.* 1990). The existence of alleles that confer some, but not other, phenotypes indicates that some of these phenotypes are genetically distinct. For instance, the *rad3-K48R* mutation blocks helicase

This work is dedicated to the memory of Brenda Knowles, scientist and friend.

Corresponding author: Adam M. Bailis, Dept. of Molecular Biology, Beckman Institute of the City of Hope, 1450 E. Duarte Rd., Duarte, CA 91010. E-mail: abailis@bricoh.coh.org

activity *in vitro* and confers sensitivity to UV light, but does not confer a growth defect (Sung *et al.* 1988). This separates the growth-control and UV-damage-repair functions of Rad3p and indicates that Rad3p helicase activity is not required for growth control. Further, it suggests that Rad3p may perform more than one biochemical function.

We previously isolated the *rad3-G595R* mutant on the basis of its temperature-sensitive growth phenotype and elevated levels of SRR (Bailis *et al.* 1995). Interestingly, the *rad3-G595R* mutation increased the frequency of recombination between short sequences but not long sequences. This suggests that the effect of *rad3-G595R* on SRR is distinct from the previously identified *rem* phenotype where spontaneous recombination between sequences in excess of 300 bp is affected (Montelone *et al.* 1988; Song *et al.* 1990).

Physical studies of recombination in the *rad3-G595R* mutant suggested a link between the SRR phenotype and defective processing of the ends of broken DNA molecules (Bailis *et al.* 1995). We found that degradation of both the 5' and 3' strands is slower in this mutant. This led us to propose that reduced exonucleolytic processing allows sequences adjacent to a break to persist, increasing the likelihood of recombination with similar sequences in the genome.

We demonstrated the link between the SRR- and DNA-processing phenotypes in a subsequent study (Bailis and Maines 1996). We found that adding heterologous DNA onto the ends of a DNA fragment with little terminal homology to the *HIS3* locus blocked insertion into the *HIS3* locus in *rad3-G595R* mutant cells, but not wild-type cells. In this case, blocking degradation of the ends of broken DNA inhibited the removal of heterologous sequences obscuring the homologous sequences on the fragment, preventing recombination. This is consistent with *rad3-G595R* affecting SRR by changing the processing of broken DNA molecules. Further, it suggests that the amount of degradation in wild-type cells is usually sufficient to degrade any short repeats that may flank a break. This could reduce the incidence of SRR by leaving unique sequence DNA at the break that can be healed by recombination with sequences on a sister chromatid or homolog without rearranging the genome. Because the length of the unique sequences separating dispersed, short repeats tends to exceed the repeat length (Rothstein 1979), breaks terminating in these regions should be repaired relatively efficiently.

In this report we present evidence that the role played by *RAD3* in SRR control is distinct from its roles in UV resistance and mutation avoidance. We also discuss the isolation of an allele of the *SSL1* gene, *SSL1-T242I*, that disrupts SRR control, but suppresses the defective transcription, growth, and SRR phenotypes conferred by *rad3-G595R*. The *SSL1* gene product, a zinc finger protein (Yoon *et al.* 1993; Humbert *et al.* 1994) and component of the heteropentamer (Feaver *et al.* 1993), has

been shown by others to interact with itself, Rad3p, and Tfb1p (Bardwell *et al.* 1994; Matsui *et al.* 1995), a third subunit of the heteropentamer (Gileadi *et al.* 1992; Feaver *et al.* 1993). Interestingly, the results of two hybrid experiments suggest that the *rad3-G595R* and *SSL1-T242I* mutations may lead to changes in how subunits of the heteropentamer interact. We speculate that the growth, transcription, and SRR phenotypes of the *rad3-G595R* and *SSL1-T242I* mutants may all be due to changes within the heteropentamer.

MATERIALS AND METHODS

Strains: The yeast strains constructed for this study are isogenic, derived from W303-1A and W303-1B (Thomas and Rothstein 1989), and listed in Table 1. The two-hybrid strains CTY10-5d and Y187 were the gifts of Stan Fields and Steve Elledge, respectively. Standard methods were used for the growth, maintenance, and genetic manipulation of yeast (Sherman *et al.* 1986). Both the spheroplast (Hinnen *et al.* 1978) and alkali cation (Ito *et al.* 1983) methods of yeast transformation were employed.

Plasmids: The plasmids used in this study are listed in Table 2 and were built using standard molecular biological methods (Maniatis *et al.* 1989). All enzymes were obtained from New England Biolabs (Beverly, MA). All chemicals were obtained from Sigma (St. Louis, MO). pRS414 and 416 were kindly provided by Phil Hieter (Christiansen *et al.* 1991). pGHOT (Nickoloff *et al.* 1986) was generously provided by Jac Nickoloff and Fred Heffron. p1032 and 1033 were the kind gifts of Tom Donahue (Yoon *et al.* 1993). The two-hybrid plasmids pBTM116, pGAD-HB, pBTMRAD3, pGADSSL1, pMASSL1, pGADTFB1, and pMATFB1 were the generous gifts of Lee Bardwell (Bardwell *et al.* 1994).

Mutagenesis and selection for suppressors of the temperature-sensitive growth phenotype of a *rad3-G595R* mutant: A temperature-sensitive *rad3-G595R* mutant strain, ABX46-1C, was mutagenized to 20–30% viability with ethyl methanesulfonate. Approximately 200,000 survivors were plated onto YPD (2% dextrose, 2% bacto-peptone, 1% yeast extract) plates and incubated at the nonpermissive temperature of 37° for 5 days to select for high-temperature-resistant mutants.

RNA isolation and Northern blot hybridization: Wild-type and mutant cells were grown to midlog ($1-5 \times 10^7$ cells/ml) in 10 ml of YPD liquid medium at 30°. The cultures were split and one half incubated at 30° and the other half at 37° for 1 hr. The cells from both cultures were harvested and washed, and total cellular RNA was prepared as described previously (Elion and Warner 1984). RNA (10 µg) was denatured and loaded into each lane of a 1.2% agarose, 3% formaldehyde, 20 mM *N*-morpholinopropanesulfonic acid (MOPS), and 1 mM EDTA gel and electrophoresed. Size-fractionated RNA was transferred to a nylon membrane and hybridized with both a 1.2-kb *HindIII/HindIII URA3* sequence and a 590-bp *SaI/SnaBI SAM1* fragment that had been ³²P-labeled by random priming. After quantitation of the *URA3* and *SAM1* hybridization signals with a phosphorimager, the blots were stripped and rehybridized with a ³²P-labeled 330-bp double-stranded DNA probe specific for 18S rRNA. These signals were used to normalize the *URA3* and *SAM1* levels because rRNA levels are unaffected by the *rad3-G595R* and *SSL1-T242I* mutations (T. Negritto and A. Bailis, unpublished data).

Growth-rate determination: YPD liquid (5 ml) was inoculated with a single yeast colony and grown to saturation at 30°. The saturated cultures were used to inoculate 25 ml of

TABLE 1
***S. cerevisiae* strains**

Strain	Genotype ^a
W303-1B	<i>MATα</i>
W961-5A	<i>MATa HIS3</i>
ABM43	<i>MATa TRP1 rad3-G595R SSL1-T242I</i>
ABM47	<i>MATa HIS3 rad3-20</i>
ABT84	<i>MATα sam1-ΔBgl II SSL1::URA3::SSL1-1</i>
ABT88	<i>MATα SSL1-T242I::URA3::SSL1</i>
ABT151	<i>MAT::LEU2 pLAY97 (URA3, HOcs) pGHOT (TRP1, GAL1::HO)</i>
ABT152	Same as ABT151 except <i>rad3-G595R</i>
ABT157	Same as ABT151 except <i>SSL1-T242I</i>
ABT197	Same as ABT151 except <i>rad3-G595R, SSL1-T242I</i>
ABT198	<i>MATa/α ade2-1/- can1-100/- his3ΔHindIII/HIS3 leu2-3,112/- TRP1/trp1-1 ura3-1/- pLGSD5 (URA3, GAL1::CYC1::lacZ)</i>
ABT199	Same as ABT198 except <i>rad3-G595R/rad3-G595R</i>
ABT200	Same as ABT198 except <i>RAD3/rad3-G595R</i>
ABT204	<i>MATa ade2-1 can1-100 HIS3 leu2-3,112 trp1-1 ura3-1 pLGSD5 (URA3 GAL1::CYC1::lacZ)</i>
ABT201	Same as ABT204 except <i>rad3-G595R</i>
ABT202	Same as ABT204 except <i>rad3-G595R SSL1-T242I</i>
ABT203	Same as ABT204 except <i>SSL1-T242I</i>
ABT213	<i>MATa ade2 gal4 gal80 his3-200 leu2-3,112 trp1-901 URA3::lexA op::lacZ pBTM-RAD3 (lexA::rad3 TRP1) pGAD-SSL1 (gal4::ssl1 LEU2)</i>
ABT214	Same as ABT213 except <i>pLAY220 (lexA::rad3-G595R TRP1) pGAD-SSL1 (gal4::ssl1 LEU2)</i>
ABT216	Same as ABT213 except <i>pBTM-RAD3 (lexA::rad3 TRP1) pGAD-HB (gal4 LEU2)</i>
ABT217	Same as ABT213 except <i>pBTM116 (lexA TRP1) pGAD-HB (gal4 LEU2)</i>
ABT218	Same as ABT213 except <i>pBTM116 (lexA TRP1) pGAD-SSL1 (gal4::ssl1 LEU2)</i>
ABT219	Same as ABT213 except <i>pLAY220 (lexA::rad3-G595R TRP1) pLAY226 (gal4::ssl1-T242I LEU2)</i>
ABT220	Same as ABT213 except <i>pBTM-RAD3 (lexA::rad3 TRP1) pLAY226 (gal4::ssl1-T242I LEU2)</i>
ABT224	<i>MATα HIS3 SSL1-T242I pLAY232 (TRP1 SSL1-T242I)</i>
ABT225	<i>MATα ade2-101 gal4 gal80 his3 leu2-3,112 trp1-901 URA3::gal1::lacZ pMA-TFBI (gal4::tbf1 HIS3) pGAD-SSL1 (gal4::ssl1 LEU2)</i>
ABT226	Same as ABT225 except <i>pMA-TFBI gal4::tbf1 HIS3) pLAY226 (gal4::ssl1-T242I LEU2)</i>
ABT227	Same as ABT225 except <i>pMA-SSL1 (gal4::ssl1 HIS3) pGAD-SSL1 (gal4::ssl1 LEU2)</i>
ABT228	Same as ABT225 except <i>pMA-SSL1 (gal4::ssl1 HIS3) pLAY226 (gal4::ssl1-T242I LEU2)</i>
ABT229	Same as ABT225 except <i>pMA-SSL1 (gal4::SSL1 HIS3) pGAD-TFB1 (gal4::TFB1 LEU2)</i>
ABT249	Same as ABT225 except <i>pLAY289 (gal4::ssl1-T242I HIS3) pLAY226 (gal4::ssl1-T242I LEU2)</i>
ABX46-1C	<i>MATa TRP1 rad3-G595R</i>
ABX81-9D	<i>MATα HIS3 rad3-G595R</i>
ABX83-11D	<i>MATa HIS3 SSL1-3</i>
ABX96-8D	<i>MATα HIS3 TRP1 SSL1-T242I</i>
ABX108-5D	<i>MATa HIS3 SSL1-T242I</i>
ABX131-2A	<i>MATα HIS3 rad3-G595R SSL1-T242I</i>
ABX139	<i>MATa/α ade2-1/- can1-100/- his3ΔHindIII/HIS3 leu2-3,112/- TRP1/trp1-1 ura3-1/-</i>
ABX140	Same as ABX139 except <i>rad3-G595R/rad3-G595R</i>
ABX141	Same as ABX139 except <i>RAD3/rad3-G595R</i>
ABX144	Same as ABX139 except <i>SSL1/SSL1-T242I</i>
ABX147	Same as ABX139 except <i>SSL1/SSL1-T242I rad3-G595R/rad3-G595R</i>
ABX152	Same as ABX139 except <i>SSL1-T242I/SSL1-T242I rad3-G595R/rad3-G595R</i>
ABX156	Same as ABX139 except <i>SSL1-T242I/SSL1-T242I</i>
ABX195-7B	<i>MATa ade2-1 can1-100 leu2-3,112 trp1-1 ura3-1 his3-5'::URA3::his3-3' (415-bp direct repeat)</i>
ABX177-4C	Same as ABX-195-7B except <i>rad3-G595R SSL1-T242I</i>
ABX177-10D	Same as ABX-195-7B except <i>SSL1-T242I</i>
ABX197-2A	Same as ABX-1957B except <i>rad3-G595R</i>
ABX192-1A	<i>MATa ade2-1 can1-100 leu2-3,112 trp1-1 ura3-1 his3-5'::URA3::his3-3' (223-bp direct repeat)</i>
ABX178-7A	Same as ABX192-1A except <i>rad3-G595R, SSL1-T242I</i>
ABX178-16B	Same as ABX192-1A except <i>SSL1-T242I</i>
ABX198-1B	Same as ABX192-1A except <i>rad3-G595R</i>
ABX212-14B	<i>MATα ade2-1 can1-100 leu2-3,112 trp1-1 ura3-1 his3-5'::URA::his3-3' (103-bp direct repeat)</i>
ABX213-3B	Same as ABX212-14B except <i>rad3-G595R</i>
ABX222-24A	Same as ABX212-14B except <i>SSL1-T242I</i>
ABX222-11A	Same as ABX212-14B except <i>rad3-G595R SSL1-T242I</i>

^a All strains possess the following genotype except where noted: *ade2-1 can1-100 his3-11, 15 leu2-3,112 trp1-1 ura3-1*. W303-1B was provided by R. Rothstein, and W961-5A was provided by J. McDonald. All other strains were developed for this study.

YPD liquid to a density of 5×10^6 to 1×10^7 cells/ml and were grown at 30°. Culture density was assessed at 30-min intervals by turbidimetry using a Klett-Summerson colorimeter fitted with a red filter.

UV sensitivity assays: Five-milliliter YPD liquid cultures were started from single colonies and grown to saturation at 30°. Appropriate dilutions were plated onto YPD plates and exposed to varying doses of UV light in a UV cross-linker (Stratagene, La Jolla, CA). Irradiated cells were incubated in the dark at 30° for 3–5 days and the number of surviving colonies counted. The fraction of cells surviving treatment was determined by dividing the number of colonies formed after exposure by the number of colony-forming units in the original culture.

Mutation frequency determination: YPD medium (10 ml) was inoculated with single colonies of cycloheximide-sensitive yeast and grown to saturation at 30°. The cells were harvested, washed, and resuspended in water. Cells were plated onto YPD agar plates containing 10 µg/ml cycloheximide, a dose that selects primarily for mutations in the *CYH2* ribosomal protein gene (Sikorski and Boeke 1991). The number of cycloheximide-resistant colonies was counted after incubation at 30° for 5–7 days. Viable counts were determined by counting the colonies that arose on YPD plates after incubation at 30° for 2–3 days. Mutation frequencies were determined by dividing the number of cycloheximide-resistant mutant colonies by the number of viable cells plated. Median mutation frequencies were determined from at least nine independent trials. Statistical significance was tested by determining the number of trials with each strain that were above and below the grouped median frequency and then performing contingency χ^2 analysis and Yate's correction for continuity (Cochran 1954).

Galactose-inducible transcription assays: A version of a standard β -galactosidase assay was used (Miller 1972). Cells freshly transformed with pLGS5 (Table 2) were grown to midlog ($\sim 2 \times 10^7$ cells/ml) at 30° in 20 ml of uracil-less, 3% glycerol, and 3% lactate growth medium. This medium selects for the presence of the plasmid and neither induces nor represses expression of the galactose-inducible *GAL::cyc1::lacZ* fusion gene on pLGS5. The cultures were split and 1 ml of 20% (w/v) galactose was added to each culture. One culture was maintained at 30°, while the other was shifted to 37°. Both were incubated for 1 hr before harvest by centrifugation, resuspension with 1 ml of Z buffer (0.1 M Tris HCl, pH 8.0, 20% (v/v) glycerol, 1 mM dithiothreitol), disruption with glass beads, and clarification by centrifugation at 4° in a microcentrifuge for 5 min. Another 0.5 ml of Z buffer was added to the clarified extract. Cell extract (100 µl) was added to 0.9 ml of Z buffer and warmed at 37° for 5 min before addition of 0.25 ml of 4 mg/ml *o*-nitrophenylgalactoside and incubation for 15 min to 1 hr at 37°. The reactions were stopped with the addition of 0.5 ml of 1 M sodium carbonate and the amount of product released was determined spectrophotometrically by the absorbance at 420 nm. Specific activities were determined by calculating the moles of nitrophenol released per minute per milligram of protein. Protein concentration was measured using the Bio-Rad protein assay (Hercules, CA).

Two-hybrid assays: Freshly transformed cells containing the two-hybrid constructs were grown to a density of $1-7 \times 10^7$ cells/ml at 30° in 5 ml of medium that selected for the presence of the plasmids and contained 2% glucose. Cell extracts were prepared and assayed as above.

Deletion assay: Integrating pLAY202, pLAY204, or pLAY214 into the *HIS3* locus created 415-, 223-, and 103-bp duplications of *HIS3* coding sequence flanking the 5-kb plasmid YIp5. The duplication strains were maintained on uracil-less medium, which selects against loss of the *URA3* marker in YIp5. Uracil-

less medium was inoculated with a single colony and grown to saturation at 30°. Maintaining selection during growth reduces the incidence of jackpot events early in the growth of the culture, which skew the determination of recombination frequency. Cells were plated onto uracil-less agar and incubated at 30° for 5 days to determine the number of viable cells in the culture. Cells were also plated onto histidine-less medium and incubated at 30° for 5 days to select for recombinants that had generated an intact *HIS3* gene. Loss of the plasmid in the His⁺ recombinants was confirmed by replica plating to uracil-less medium and Southern blot analysis (S. Maines and A. Bail is, unpublished results). Deletion frequencies are expressed as the number of His⁺, Ura⁻ recombinants per viable cell plated. We tested for statistically significant differences between the median deletion frequencies using contingency χ^2 analysis and Yate's correction for continuity (Cochran 1954) as described above for the mutation frequencies.

DNA fragment integration assay: The plasmid pLAY144, which contains the *HIS3* gene on a 1.3-kb genomic fragment disrupted by the insertion of the *URA3* gene on a 1.2-kb fragment, was digested with a variety of restriction endonucleases to yield fragments with different lengths of *HIS3* sequence flanking the *URA3* gene. Gel-purified DNA fragments were used to transform His⁺ Ura⁻ yeast spheroplasts to uracil prototrophy. The number of uracil prototrophs was counted, and all were screened for the ability to grow without histidine to determine whether the DNA fragments had integrated into, and disrupted, the *HIS3* locus (Ura⁺ His⁻) or gene-converted the *ura3-1* marker at the *URA3* locus (Ura⁺ His⁺). Southern blots of over 100 Ura⁺ recombinants showed that the DNA fragments either integrated at the *HIS3* locus or gene-converted the *ura3-1* marker at the *URA3* locus (S. Maines and A. Bail is, unpublished results). Percentage insertion of the DNA fragment into the *HIS3* locus, versus gene conversion at the *URA3* locus, was determined by dividing the number of His⁻ transformants by the total number of transformants (His⁺ and His⁻) and multiplying by 100. The efficiency of transformation with these fragments, normalized against the efficiency of transformation with an intact centromere plasmid, varied from 10- to 15-fold with changes in the length of *HIS3* homology, but only 1.5- to 4-fold from strain to strain (S. Maines and A. Bail is, unpublished results).

Double-strand break (DSB) processing assay: Stationary cultures grown from single colonies of yeast transformed with pLAY97 (Negritto *et al.* 1997) and pGHOT (Nickoloff *et al.* 1986) were used to inoculate 500 ml of medium that selected for both plasmids (without uracil or tryptophan) and neither induced nor repressed the galactose-inducible *GAL::HO* fusion gene on pGHOT (3% glycerol, 3% lactate). Cultures were grown to a density of 5×10^8 cells/ml at 30° before a 50-ml aliquot was removed, the cells were pelleted, and the pellet was frozen at -80°. Fifty milliliters of 20% galactose was then added to the culture to induce expression of the *GAL::HO* gene on pGHOT, which cut at the unique HO recognition site in pLAY97. Induction proceeded for 30 min at 30°, at which time hemacytometer counts were made, another aliquot was removed, and the cells were processed as above. The cells were then filtered free of this medium through sterile 0.4-µm nitrocellulose filters and resuspended in fresh, prewarmed, minimal medium lacking tryptophan and containing 2% glucose. Uracil was provided because pLAY97 was cleaved in more than 50% of the cells exposed to these conditions and less than 1% of the broken plasmids rejoin (Bail is and Maines 1996). Glucose was provided to repress *GAL::HO* gene expression. Cells were counted and aliquots removed and processed at regular intervals as described above.

Total cellular DNA was prepared from the frozen cell pellets by a standard protocol (Hoffman and Winston 1987), di-

TABLE 2
Plasmids

Plasmid	Description	Reference
pI032	4.2-kb BamHI/EcoRI genomic clone containing the SSL1-2 allele in YCp50.	Yoon et al. (1993)
pI033	4.2-kb BamHI/EcoRI genomic clone containing the SSL1-3 allele in YCp50.	Yoon et al. (1993)
pRS414	pBluescript modified by the addition of a yeast centromere and a TRP1 marker.	Christiansen et al. (1991)
pRS416	pBluescript modified by the addition of a yeast centromere and a URA3 marker.	Christiansen et al. (1991)
pLGSD5	GAL1::CYC1::lacZ fusion facilitates inducible β -galactosidase expression.	Schneider and Guarente (1991)
pGHOT	GAL1::HO fusion facilitates inducible HO-endonuclease expression.	Nickoloff et al. (1986)
pBTMRAD3	RAD3 coding sequence fused to sequence coding for DNA binding domain of lexA.	Bardwell et al. (1994)
pMASSL1	SSL1 coding sequence fused to sequence coding for DNA binding domain of GAL4.	Bardwell et al. (1994)
pMATFB1	TFB1 coding sequence fused to sequence coding for DNA binding domain of GAL4.	Bardwell et al. (1994)
pGADSSL1	SSL1 coding sequence fused to sequence coding for activation domain of GAL4.	Bardwell et al. (1994)
pGADTFB1	TFB1 coding sequence fused to sequence coding for activation domain of GAL4.	Bardwell et al. (1994)
pLAY97	117-bp HOcs fragment inserted into KpnI and XhoI cut pRS416.	Negritto et al. (1997)
pLAY144	1.2-kb BamHI/BamHI URA3 sequence inserted into the BglII cut HIS3 sequence on a 1.3-kb genomic clone. Replaces 70-bp of HIS3 coding sequence with URA3.	Bails and Maines (1996)
pLAY158	1.0-kb XhoI/BamHI fragment containing a his3 allele with 187-bp of the coding sequence removed and inserted into Sall/BamHI cut Yip5.	This study
pLAY159	413-bp XhoI/AflIII lacI fragment from pBluescript inserted into pGEM2	This study
pLAY169	4.2-kb BamHI/EcoRI genomic clone containing SSL1 inserted into pRS416.	This study
pLAY183	SSL1-T242I sequence recovered into pLAY169 by gap repair.	This study
pLAY198	4.2-kb BamHI/EcoRI fragment containing SSL1-T242I from pLAY183 inserted into BamHI/EcoRI cut Yip5.	This study
pLAY202	415-bp KpnI/MscI HIS3 coding sequence fragment inserted into Yip5.	This study
pLAY204	227-bp KpnI/BglII HIS3 coding sequence fragment inserted into Yip5.	This study
pLAY214	103-bp BstBI/NheI HIS3 coding sequence fragment inserted into Yip5.	This study
pLAY220	Swap 1.2-kb MscI/SpeI fragment containing rad3-G595R mutation with equivalent RAD3 wild-type fragment in pBTMRAD3	This study
pLAY226	Swap 150-bp NdeI/StuI fragment containing SSL1-T242I mutation with equivalent SSL1 wild-type fragment in pGADSSL1	This study
pLAY232	4.2-kb BamHI/EcoRI fragment containing SSL1-T242I from pLAY183 inserted into BamHI/EcoRI cut pRS414	This study
pLAY289	Swap 150-bp NdeI/StuI fragment containing SSL1-T242I mutation from pLAY183 with equivalent SSL1 wild-type fragment in pMASSL1	This study

gested with *ScaI* restriction endonuclease, blotted to nylon, and probed with ³²P-labeled pBluescript DNA, which is the backbone of pLAY97. The patterns of hybridization were visualized and quantitated with a Molecular Dynamics phosphorimager. DSB processing was quantitated by comparing the levels of the 2.8- and 3.4-kb *ScaI* and HO cut bands with those of the *ScaI* cut 6.2-kb band. Signal levels were not much influenced by the outgrowth of cells in which pLAY97 was not cut because all cells required at least 4 hr to double in density (Bailis *et al.* 1995; S. Maines and A. Bailis, unpublished results), when the broken plasmid signal was reduced at least eightfold (see results). Further, while the wild type and *SSL1-T242I* doubling times were very similar, the kinetics of DSB processing were very different (see results).

DNA from each time-point was transferred to a positively charged nylon membrane under either denaturing (0.4 N sodium hydroxide) or nondenaturing (3 M sodium chloride, 0.3 M sodium citrate, pH 7.0) conditions using a slot blot manifold (Bio-Rad, Hercules, CA) and fixed to the membrane using a UV cross-linker. The blots were hybridized with a ³²P-labeled 413-base RNA species complementary to one side of the HO cut-site in pLAY97, obtained by *in vitro* transcription of pLAY159. Hybridization signals were quantitated with a phosphorimager. Levels of single-stranded DNA were determined by dividing the nondenatured DNA signals by the denatured DNA signals.

RESULTS

A mutation in *SSL1* suppresses the *rad3-G595R* temperature-sensitive growth defect: Approximately 6×10^5 *rad3-G595R* mutant cells (ABX46-1C) were mutagenized to 30% survival with EMS, plated onto YPD agar, and incubated at 37° to select for mutants that suppress the temperature-sensitive growth defect. Three high-temperature-resistant clones were isolated and crossed to a wild-type strain (W961-5A). All three of the suppressors segregated as single genes, one linked to the *RAD3* locus, and the other two unlinked to *RAD3*. One of the extragenic suppressors gave variable suppression of the *rad3-G595R* growth phenotype and was not studied further, while the other extragenic suppressor consistently suppressed the *rad3-G595R* growth defect. A cross between this strain (ABM43) and a *rad3-G595R* mutant (ABX81-9D) determined that the suppressor is dominant because the resulting diploid grew at 37°. The suppressor was discovered to confer a mild temperature-sensitive growth defect when it segregated away from the *rad3-G595R* mutation in crosses to wild type. The isolated suppressor was backcrossed five more times to wild type. All putative suppressor-containing segregants were checked for the ability to suppress the *rad3-G595R* Ts growth phenotype in crosses.

We reasoned that because the temperature-sensitive phenotype of the *rad3-ts₁₄* allele is linked to a transcription defect (Guzder *et al.* 1994), the same may be true for *rad3-G595R*. Further, because the *RAD3* gene exerts its effect on transcription through TFIIH (Feaver *et al.* 1993), the suppressor mutation might be in a gene that codes for another subunit of TFIIH. To test this hypothesis we crossed the original suppressed *rad3-G595R* strain

(ABM43) with a strain containing a *URA3*-marked *SSL1* locus (ABT84). We looked for linkage to *SSL1* because the Rad3p and Ssl1p proteins interact *in vivo* and *in vitro* (Bardwell *et al.* 1994). We found that the suppressor segregated in repulsion with the *URA3* marker, indicating that the suppressor was very closely linked to the *SSL1* locus. To further define the location of the suppressor mutation, the mutant *SSL1* sequence from a suppressor strain (ABX96-8D) was recovered by gap repair (Rothstein 1991) and sequenced, revealing a single C to T transition at residue 725 that converts the threonine codon at position 242 to an isoleucine codon. Thereafter, the suppressor was referred to as *SSL1-T242I* because of the dominant nature of the suppressor phenotype.

The *rad3-G595R* and *SSL1-T242I* mutant cells display defective growth and transcription phenotypes: We were interested in quantitating the effects of the *rad3-G595R* mutation on growth and transcription. We determined that the *rad3-G595R* growth defect is recessive and is more severe at 30° than at 37° (Table 3). We also found that the *rad3-G595R* mutant has a recessive defect in expression from a galactose-inducible *CYC1::lacZ* fusion gene (2.5- to 3-fold reduced) and consistently lower steady-state levels of the *URA3* and *SAM1* mRNAs at both 30° and 37° (Table 4). These results are similar to those observed previously with the *rad3-ts₁₄* mutant mentioned above (Guzder *et al.* 1994), indicating that the *rad3-G595R* mutation may block transcription and inhibit growth in a similar way.

We also determined the effects of the *SSL1-T242I* allele on growth and transcription. We found that the mild temperature-sensitive growth phenotype conferred by *SSL1-T242I* is recessive, while the *rad3-G595R* slow growth suppressor phenotype is semi-dominant because two copies of the *SSL1-T242I* allele suppress better than one (Table 3). We also found that the *SSL1-T242I* mutant exhibits small, but significant, increases in *CYC1::lacZ* fusion gene expression, but no significant changes in the steady-state levels of either the *SAM1* or *URA3* mRNAs (Table 4). Interestingly, however, the *rad3-G595R SSL1-T242I* double mutant displays fusion gene expression and steady-state mRNA levels that are near wild type (Table 4), indicating that the *SSL1-T242I* mutation also suppresses the transcription defect conferred by *rad3-G595R*.

***rad3-G595R* and *SSL1-T242I* have minimal effects on mutation avoidance and UV resistance:** Because other hyper-rec *rad3* mutants display mutator phenotypes (Montelione *et al.* 1988; Song *et al.* 1990), we investigated whether the *rad3-G595R* mutant also displays elevated levels of spontaneous mutation. We determined that the mutation frequency in *rad3-G595R* cells (4.2×10^{-9} mutations/viable ABX81-9D cell) is not statistically different ($P = 0.35$) from that of wild-type cells (2.7×10^{-9} mutations/viable W961-5A cell). This suggests that the recombination phenotype observed in *rad3-G595R*

TABLE 3
Growth rates

Strain	Genotype	Doubling time (min) ^a	
		30°	37°
W961-5A	WT haploid	105	85
ABX81-9D	<i>rad3-G595R</i>	190	450
ABX108-5B	<i>SSL1-T242I</i>	105	130
ABX131-2A	<i>rad3-G595R SSL1-T242I</i>	105	140
ABX139	WT diploid	130	90
ABX140	<i>rad3-G595R/rad3-G595R</i>	180	460
ABX141	<i>RAD3/rad3-G595R</i>	130	90
ABX156	<i>SSL1-T242I/SSL1-T242I</i>	135	115
ABX144	<i>SSL1/SSL1-T242I</i>	130	85
ABX152	<i>rad3-G595R/rad3-G595R SSL1-T242I/SSL1-T242I</i>	135	125
ABX147	<i>rad3-G595R/rad3-G595R SSL1/SSL1-T242I</i>	135	170

^a All strains were grown in complete synthetic medium. Cell density was determined using a Klett-Summerson colorimeter.

mutants is not related to the mutation avoidance function of *RAD3*. The mutation frequency in the *SSL1-T242I* mutant (2.0×10^{-9} mutations/viable ABX108-5B cell) is also not different from wild type ($P = 0.74$).

Several *rad3* and *ssl1* mutants that display extreme sensitivity to UV light have been isolated (Reynolds and Friedberg 1981; Wilcox and Prakash 1981; Yoon *et al.* 1993). We found that the *rad3-G595R* and *SSL1-T242I* mutant strains are nearly as resistant to UV light as wild type (Figure 1). In contrast, *rad3-20* mutant cells (Naumovski and Friedberg 1986) that possess a normal recombination phenotype (Bailis and Maines 1996) are highly UV sensitive. These results suggest that the phenotypes conferred by the *rad3-G595R* and *SSL1-T242I* mutations are not due to an NER defect.

***rad3-G595R* and *SSL1-T242I* act together to influence short-repeat recombination:** As discussed above, our work suggests that the *rad3-G595R* mutation disrupts the barrier against recombination between sequences below 250–300 bp in length (Bailis *et al.* 1995; Bailis and Maines 1996). To extend our observations we determined the frequencies of spontaneous deletion by recombination between 103-, 223-, and 415-bp nontandem repeats in wild-type and *rad3-G595R* mutant cells. If the *rad3-G595R* mutation specifically affects the control of SRR we expected that the frequency of recombination between the 415-bp repeats, which are longer than the 250- to 300-bp threshold between long- and short-repeat recombination (Jinks-Robertson *et al.* 1993), would be minimally altered. Concomitantly, we

TABLE 4
Transcription induction and steady-state mRNA levels in wild-type and mutant cells

Genotype	Steady-state mRNA levels ^b					
	β -Gal activity ^a		<i>SAM1</i>		<i>URA3</i>	
	30°	37°	30°	37°	30°	37°
WT haploid	782 \pm 52	989 \pm 90	1.0 \pm 0.03	0.69 \pm 0.03	1.10 \pm 0.02	0.23 \pm 0.1
<i>rad3-G595R</i>	257 \pm 7	393 \pm 28	0.70 \pm 0.07	0.30 \pm 0.08	0.35 \pm 0.09	0.09 \pm 0.05
<i>SSL1-T242I</i>	1378 \pm 119	1600 \pm 114	1.10 \pm 0.13	0.73 \pm 0.13	1.30 \pm 0.07	0.42 \pm 0.22
<i>rad3-G595R SSL1-T242I</i>	889 \pm 11	1200 \pm 39	1.0 \pm 0.04	0.72 \pm 0.04	1.10 \pm 0.04	0.32 \pm 0.05
WT diploid	1034 \pm 21	1120 \pm 49	1.0 \pm 0.06	0.67 \pm 0.05	1.0 \pm 0.05	0.26 \pm 0.12
<i>rad3-G595R/rad3-G595R</i>	187 \pm 7	272 \pm 18	0.62 \pm 0.11	0.26 \pm 0.1	0.27 \pm 0.06	0.09 \pm 0.06
<i>RAD3/rad3-G595R</i>	1353 \pm 119	1225 \pm 134	1.10 \pm 0.1	0.67 \pm 0.14	0.90 \pm 0.29	0.24 \pm 0.14

^a β -Gal activity, expressed in Miller units (nmoles nitrophenol-released per minute per milligram of protein) was determined in the following strains as described in materials and methods: ABT204, ABT201, ABT203, ABT202, ABT198, ABT199, ABT200. The mean specific activities from at least four trials \pm 2 SE are reported. Differences of more than 2 SE are significant beyond the 95% confidence level.

^b Steady-state levels of *URA3* and *SAM1* mRNAs and 18S rRNA species at 30° and 37° were determined in the following strains as described in materials and methods: W961-5A, ABX81-9D, ABX108-5B, ABX131-2A, ABX139, ABX140, and ABX141. The values reported are the means of two or more trials \pm 2 SE.

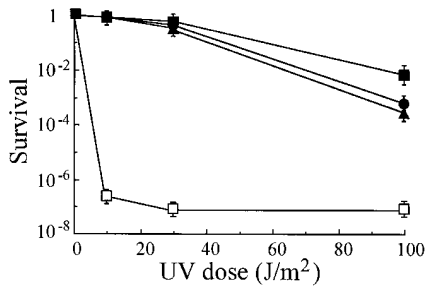


Figure 1.—Sensitivity of wild-type and mutant *S. cerevisiae* cells to UV radiation. The fraction of isogenic wild-type (solid boxes), *SSL1-T242I* (solid circles), *rad3-G595R* (solid triangles), and *rad3-20* (open squares) mutant yeast cells surviving 10, 30, or 100 J/m² doses of UV radiation was determined as discussed in materials and methods. The means ± 2 SE from at least three separate determinations are reported. Mean values that are different by >2 SE are different at the 95% confidence level.

expected that the frequency of recombination between the 223-bp repeats, which are just below the threshold length, would be more increased, while the frequency of recombination between the 103-bp repeats, which are considerably below the threshold length, would be the most increased. As expected, we found that the *rad3-G595R* mutation increases deletion frequencies 2-fold for the 415-bp repeats ($P = 0.0002$), 4-fold for the 223-bp repeats ($P = 0.0001$), and 10-fold for the 103-bp repeats ($P = 0.0001$) (Figure 2). The *SSL1-T242I* mutation has a similar but smaller effect on the control of SRR as deletion frequencies are unchanged from wild type when the repeats are 415 bp ($P = 0.73$), but are increased 2-fold for 223-bp repeats ($P = 0.02$) and nearly 3-fold for 103-bp repeats ($P = 0.005$; Figure 2). Most interestingly, however, the *rad3-G595R SSL1-T242I* double mutant displays deletion frequencies for the 415-bp ($P = 0.65$), 223-bp ($P = 0.12$), and 103-bp repeats ($P = 0.20$) that are not statistically different from wild type (Figure 2), indicating that the *rad3-G595R* and *SSL1-T242I* mutations suppress each other. These results indicate that the *rad3-G595R* and *SSL1-T242I* mutations can act together to influence SRR.

We also used an assay of DNA fragment insertion into homologous genomic sequences (Bailis and Maines 1996) to study the effects of the *rad3-G595R* and *SSL1-T242I* mutations on a different type of recombination event. Unlike the spontaneous deletion events that involve sequences that can be on the same or different molecules and are initiated at random, the insertion events involve sequences on different molecules and are initiated by the ends of the DNA fragments. However, these events may be mechanistically similar, involving the formation and resolution of heteroduplex DNA (Klein 1995; Leung *et al.* 1997; Negritto *et al.* 1997). Interestingly, we found that DNA fragment insertion increases in both *rad3-G595R* and *SSL1-T242I* mutant

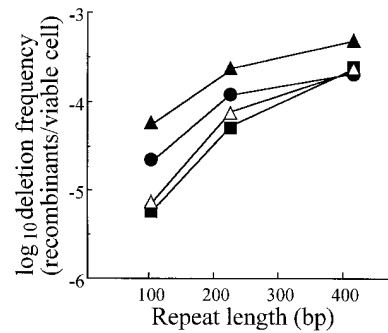


Figure 2.—Relationship between *HIS3* duplication length and frequency of deletion by direct-repeat recombination in wild-type and mutant cells. Recombination between duplicate 103-, 223-, or 415-bp *HIS3* coding segments in wild-type (solid boxes), *rad3-G595R* (solid triangles), *SSL1-T242I* (solid circles), and *rad3-G595R SSL1-T242I* (open triangles) recreates an intact *HIS3* gene and deletes a *URA3* marker as described in the text. Frequencies are expressed as the number of deletions per viable cell plated. Assays were conducted at 30°. The median frequency from a minimum of 10 separate determinations was plotted against the length of the repeat in base pairs. The statistical relationships between the median frequencies were determined using contingency χ^2 analysis with Yate's continuity correction and are discussed in the text.

cells and that the effect is greatest when the lengths of sequence shared by the fragment and genomic target were shorter than 300 bp (Figure 3). We also found that the insertion of the smallest DNA fragment in *rad3-G595R SSL1-T242I* double-mutant cells is more like wild type than either of the single mutants (Figure 3). The observation that the *rad3-G595R* and *SSL1-T242I* mutations have very similar effects on deletion and insertion suggests that they affect recombination between sequences on the same and on different molecules and, perhaps, between linked and unlinked repeats (Bailis *et al.* 1995).

When recombination between short sequences in *SSL1-T242I* mutant strains was studied, we observed unusual genetic interactions when more than one copy of the *SSL1-T242I* allele was present in the cell. First, we found that DNA fragment insertion with short homologies is elevated in *SSL1-T242I* haploids and *SSL1/SSL1-T242I* heterozygous diploids, but wild type in *SSL1-T242I/SSL1-T242I* homozygous mutant diploids (Table 5). Therefore, one *SSL1-T242I* mutant allele in a diploid cell confers a mutant recombination phenotype, indicating that this allele is dominant, while the presence of a second allele suppresses the dominant effect. This unusual gene dosage effect is also observed in *SSL1-T242I* haploid cells that contain another *SSL1-T242I* gene on a single-copy plasmid (Table 5). Interestingly, *SSL1-3*, an allele isolated on the basis of its effect on translational pausing at RNA secondary structure (Yoon *et al.* 1993), also confers an elevated insertion phenotype in a haploid mutant (Table 5) and a wild-type phenotype

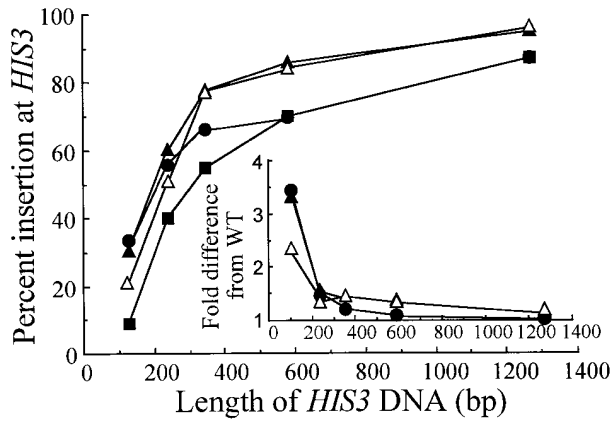


Figure 3.—An assay of the insertion of DNA fragments into the genome by homologous recombination. Isogenic wild-type (solid boxes), *rad3-G595R* (solid triangles), *SSL1-T242I* (solid circles), and *rad3-G595R SSL1-T242I* (open triangles) mutant $Ura^- His^+$ spheroplasts were transformed to uracil prototrophy with 0.01–10 μ g of one of several DNA fragments containing the complete *URA3* gene on a 1.2-kb fragment flanked by the following lengths of *HIS3* DNA in base pairs: 1271 (866-bp 5' flank + 405-bp 3' flank), 583 (178-bp 5' flank + 405-bp 3' flank), 345 (178-bp 5' flank + 167-bp 3' flank), 238 (71-bp 5' flank + 167-bp 3' flank), or 127 (91-bp 5' flank + 36-bp 3' flank). All assays were conducted at 30° as discussed in materials and methods. The percentage of insertions at *HIS3* (versus gene conversions at *URA3*) was determined from a minimum of 200 transformants and plotted against the total length of *HIS3* homology in base pairs on the DNA fragment. All percentages were determined to be significantly different from wild type by contingency χ^2 analysis except for the *SSL1-T242I* percentages obtained with the two largest fragments. Inset: Fold difference between percentages of integration events at the *HIS3* locus in wild-type and mutant strains vs. length of *HIS3* homology.

in the homozygous mutant diploid (strain X73; see Bailis *et al.* 1995). Results described below suggest that this unusual phenotypic display may be due to altered interactions between subunits of the heteropentamer. This property of the *SSL1-T242I* and *SSL1-3* alleles will be discussed further in a later section.

Changes in DSB processing in *rad3-G595R* and *SSL1-T242I* mutant cells are consistent with a degradative mechanism for the control of short-repeat recombination: We have previously discussed the link between the SRR- and DSB-processing phenotypes in *rad3-G595R* mutants (Bailis *et al.* 1995; Bailis and Maines 1996). Here we show that *rad3-G595R* and *SSL1-T242I* mutants display nearly identical DSB-processing defects because the half-life of the *in vivo* linearized plasmid in both mutants (85 min) is more than twice the half-life in wild type (40 min; Figure 4B). When we monitored the appearance and persistence of 3' single-stranded DNA tails at the ends of the broken plasmids, we found a reduced rate of degradation of both the 5' and 3' strands in *rad3-G595R* and *SSL1-T242I* mutant cells (Figure 4C). For instance, 60 min are required to see the maximum amount of 3' single-stranded DNA in the *rad3-G595R* and *SSL1-T242I* mutants while only 30 min are required in wild type. Similarly, the half-life of the 3' single-stranded DNA is 150 min in wild type, but 215 min in the *SSL1-T242I* mutant and more than 240 min in the *rad3-G595R* mutant.

Most interestingly, however, we found that the DSB-processing phenotype in the *rad3-G595R SSL1-T242I* double mutant is very similar to wild type, as HO-digested plasmid DNA has a half-life of only 40 min in both strains (Figure 4B). Similarly, the amount of time required to see the maximum amount of 3' single-

TABLE 5
DNA fragment insertion into a genomic target by homologous recombination in wild-type and mutant cells

Strain	Genotype	% $Ura^+ His^+$	% $Ura^+ His^-^a$
W961-5D	WT haploid	91 (302)	9 (29)
ABX81-9D	<i>rad3-G595R</i>	70 (178)	30 (73)*
ABX96-8D	<i>SSL1-T242I</i>	69 (217)	31 (98)*
ABX83-11D	<i>SSL1-3</i>	58 (208)	42 (149)*
ABX131-2A	<i>rad3-G595R SSL1-T242I</i>	80 (182)	20 (46)*
ABT224	<i>SSL1-T242I/pLAY214 (SSL1-T242I)</i>	87 (229)	13 (36)
ABX139	WT diploid	93 (555)	7 (39)
ABX140	<i>rad3-G595R/rad3-G595R</i>	87 (254)	13 (38)*
ABX141	<i>RAD3/rad3-G595R</i>	89 (225)	11 (29)*
ABX156	<i>SSL1-T242I/SSL1-T242I</i>	93 (358)	7 (25)
ABX144	<i>SSL1/SSL1-T242I</i>	87 (260)	13 (38)*

^a All strains were transformed with the shortest DNA fragment described in the legend to Figure 3. The diploids possessed one wild-type *HIS3* allele and one allele missing all of the *HIS3* information on the DNA fragment. The percentage of transformants that were due to fragment insertion at the *HIS3* locus ($Ura^+ His^-$), or gene conversion at the *URA3* locus ($Ura^+ His^+$) was determined as described in the text. The numbers of transformants in each category are in parentheses. * Insertion percentages significantly different from wild type as determined by contingency χ^2 analysis with continuity correction.

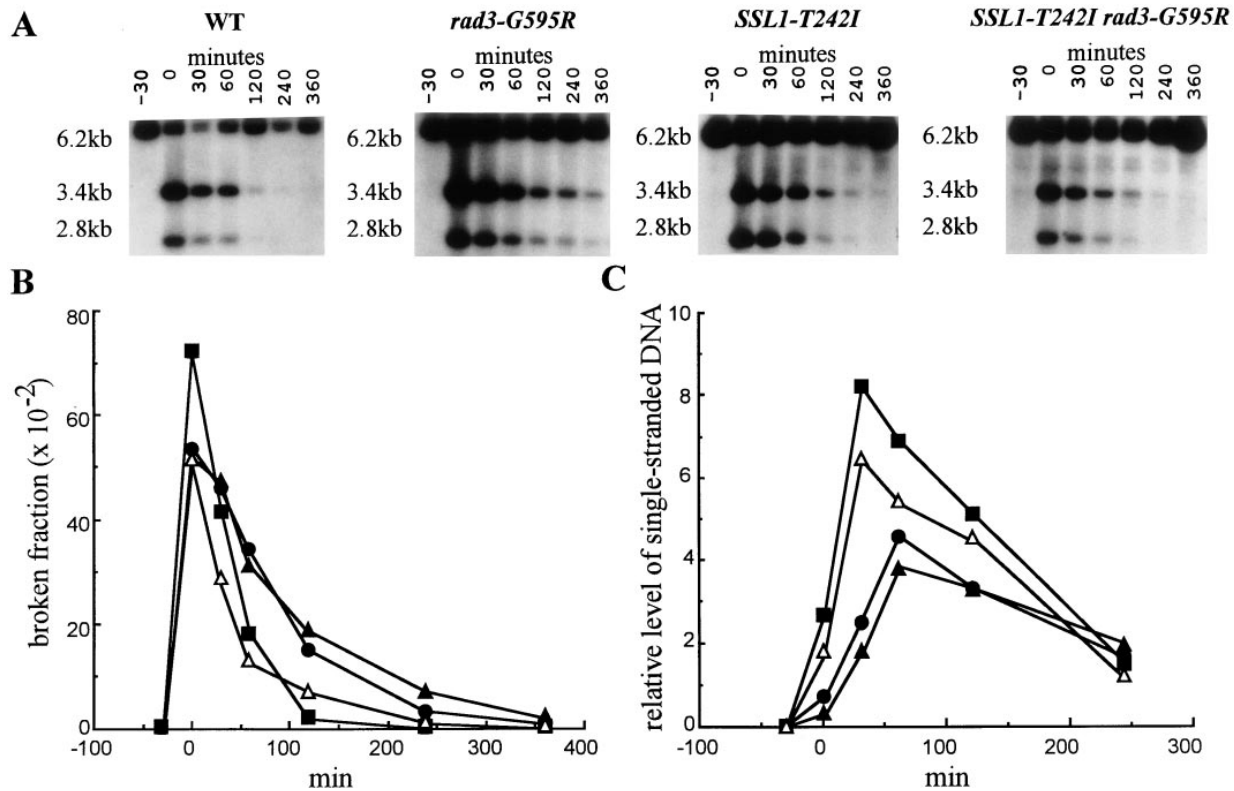


Figure 4.—Physical stability of a plasmid linearized *in vivo*. (A) Autoradiographs of plasmid DNA linearized *in vivo*. DNA was prepared from isogenic wild-type and mutant strains containing the plasmids pLAY97 and pGHOT either before a 30-min induction of HO-endonuclease expression (–30 min) or after HO-endonuclease expression was shut off (0–360 min). The autoradiogram pictures pLAY97 uncleaved by HO-endonuclease (6.2-kb band) and after HO-endonuclease cleavage (2.8- and 3.4-kb bands) as described in the text. The stability of the HO-cleaved plasmid DNA over time is indicated by changes in the intensity of the 2.8- and 3.4-kb bands relative to the 6.2-kb band. (B) Kinetics of processing linearized plasmid DNA. The kinetics of the loss of pLAY97 sequences over time from isogenic wild-type (solid squares), *rad3-G595R* (solid circles), *SSL1-T242I* (open triangles), and *rad3-G595R SSL1-T242I* (open squares) mutant strains was determined by dividing the sum of the 2.8- and 3.4-kb HO-endonuclease cut pLAY97 signals by the total pLAY97 signal obtained by summing the 6.2-kb uncut pLAY97 signal with the 2.8- and 3.4-kb cut signals and plotting the values (broken fraction) relative to elapsed time. Signal levels were determined using a phosphorimager. (C) Kinetics of single-stranded DNA formation and degradation. Slot blots were prepared from native and alkaline denatured DNA obtained from wild-type and mutant cells as described in materials and methods. The DNA was hybridized with a 413-bp single-stranded RNA probe as described in materials and methods. The signals obtained by hybridization were measured directly with a phosphorimager. The level of ssDNA at each time-point was determined by dividing the signal from the nondenatured DNA by the signal from the denatured DNA. These data were plotted vs. the time that the sample was collected.

stranded DNA in the double mutant (30 min) is the same as in wild-type cells and half the time required in both single mutants (Figure 4C), indicating that 5' strand rescission is like wild type in the double mutant. We also observed that the half-life of the 3' single-stranded DNA requires less time (175 min) in the double mutant than in either single mutant (Figure 4C), indicating that degradation of the 3' single strand is nearly normal. These data indicate that *rad3-G595R* and *SSL1-T242I* suppress each other's effects on DSB processing. Further, we suggest that *rad3-G595R* and *SSL1-T242I* work together to influence SRR by affecting the stability of broken DNA sequences.

The *rad3-G595R* and *SSL1-T242I* mutations alter interactions between Rad3, Ssl1, and Tfb1 fusion proteins in two-hybrid experiments: Bardwell *et al.* (1994) used the two-hybrid system (Fields and Song 1989) to study

interactions between wild-type Rad3p, Ssl1p, and Tfb1p and found that Ssl1p interacts with Rad3p, Tfb1p, and itself. We investigated whether the *rad3-G595R* and *SSL1-T242I* mutations alter these interactions by swapping restriction fragments containing the *rad3-G595R* and *SSL1-T242I* mutations into the Rad3 and Ssl1 two-hybrid fusion plasmids. Our data indicate that both the *rad3-G595R* and *SSL1-T242I* mutations alter interactions between the fusion proteins. First, we found that the *rad3-G595R* mutation abolishes the interaction between the Rad3 and Ssl1 fusion proteins (Table 6). Western blots of protein extracts from these cells revealed that the loss of β -galactosidase activity caused by the *rad3-G595R* mutation is not due to an inability to express the *lexA::rad3-G595R* fusion gene (G. Manthey and A. Bailis, unpublished results). This suggests that the phenotypes conferred by the *rad3-G595R* mutation

TABLE 6
Quantitative assessment of protein interaction as represented by β -galactosidase activity

Strains	Plasmids ^a		β -Gal activity (fold increase over control) ^b
	DNA-binding domain	Activation domain	
ABT217	pBTM116	pGAD-HB	—
ABT216	pBTMRAD3	pGAD-HB	1.0
ABT218	pBTM116	pGADSSL1	1.0
ABT213	pBTMRAD3	pGADSSL1	13.0
ABT214	pBTMrad3-G595R	pGADSSL1	1.0
ABT219	pBTMrad3-G595R	pGADSSL1-T242I	1.0
ABT220	pBTMRAD3	pGADSSL1-T242I	26.3
ABT225	pMATFB1	pGADSSL1	68.4
ABT229	pMASSL1	pGADTFB1	13.4
ABT226	pMATFB1	pGADSSL1-T242I	294.0
ABT227	pMASSL1	pGADSSL1	3.7
ABT228	pMASSL1	pGADSSL1-T242I	4.5
ABT249	pMASSL1-T242I	pGADSSL1-T242I	23.8

^a DNA fragments containing mutant sequences were swapped with wild-type sequences in the fusion plasmids so that mutant fusion proteins could be produced.

^b The fold increases in enzyme activity were obtained by dividing the mean activity value from each strain by the mean activity obtained with the control strain (ABT217). The means were determined from the results of a minimum of two trials.

may result from a change in the interaction between Rad3p and Ssl1p. Interestingly, Ssl1-T242I mutant fusion protein does not interact with Rad3-G595R mutant fusion protein, indicating that the suppressor mutation cannot suppress the failure of Rad3-G595R mutant fusion protein to interact with Ssl1 fusion protein.

However, the *SSL1-T242I* mutation does have several interesting effects on the behavior of the Ssl1 fusion protein (Table 6). The Ssl1-T242I mutant and wild-type Rad3 fusion proteins interact twofold better than the wild-type Ssl1 and Rad3 fusion proteins. The Ssl1-T242I fusion protein also interacts with the wild-type Tfb1 fusion protein fourfold better than does the wild-type Ssl1 fusion protein. However, the most interesting effect of the *SSL1-T242I* mutation is the interaction between two Ssl1-T242I mutant fusion proteins, sixfold greater than that between two wild-type Ssl1 fusion proteins or between wild-type Ssl1 and mutant Ssl1-T242I fusion proteins. This suggests that Ssl1-T242I mutant proteins have a significantly higher affinity for each other than do wild-type Ssl1 proteins. These results suggest that the mechanism by which the *SSL1-T242I* mutation suppresses the phenotypes conferred by the *rad3-G595R* mutation may be the result of changes in several protein-protein interactions within the heteropentamer. These interactions may also help explain the unusual gene dosage effect of the *SSL1-T242I* allele observed in the DNA fragment insertion assays (Table 5) as discussed below.

DISCUSSION

Data from our laboratory indicate that recombination between short, repeated sequences is controlled differ-

ently from recombination between longer sequences in *S. cerevisiae*. In this article we show that deletions by recombination between short repeats are more stimulated by the *rad3-G595R* mutation than deletions between longer sequences (Figure 2). In addition, we show that a newly isolated allele of the *SSL1* gene, *SSL1-T242I*, also selectively stimulates deletions (Figure 2) and DNA fragment insertions by SRR (Figure 3), but together with *rad3-G595R* it suppresses SRR (Figures 2 and 3). Together these observations show that the control of different recombination events involving short sequences can be affected by a dialog between the *RAD3* and *SSL1* genes. It is, perhaps, also indicative of the involvement of the heteropentameric core of both TFIID and the NER complex in the control of SRR.

The concordance of the DNA fragment insertion and deletion data indicates that they are under the common control of *RAD3* and *SSL1* and that this control may impinge upon all SRR. These results were presaged by the work of Jinks-Robertson *et al.* (1993), which showed that the minimum length of DNA sequence necessary to give efficient recombination is similar regardless of where the repeats are located. One clue as to how this may be accomplished was revealed by the DSB-processing phenotype observed in the *rad3-G595R* and *SSL1-T242I* mutants. We found that the ends of broken DNA molecules are more stable in *rad3-G595R* and *SSL1-T242I* single mutants than in wild type or the *rad3-G595R SSL1-T242I* double mutant (Figure 4). This is coincident with the increased SRR observed in the single mutants and lower levels of SRR in wild-type and double-mutant cells (Figures 2 and 3). More detailed analysis showed that the stability of both the 5' and 3' strands is increased in the *rad3-G595R* and *SSL1-T242I*

mutants (Figure 4), indicating, as discussed previously (Bailis *et al.* 1995), that reduced exonucleolytic processing delays degradation of short-repeat sequences adjacent to these ends, increasing the likelihood that they will be rescued by recombination.

By what mechanism are the *rad3-G595R* and *SSL1-T242I* mutations affecting the processing of DNA ends and, thereby, the control of SRR? Sancar (1994) has speculated that the helicase activity of the *RAD3* gene product may be required to open DNA duplexes around DNA lesions to provide access to nucleases that cleave on either side. Perhaps the heteropentamer is involved in separating DNA strands at the site of a nick or a break, facilitating processing by an exonuclease(s). A loss of strand-separating activity in *rad3-G595R* and *SSL1-T242I* mutant cells may explain their defective control of SRR. Because the *rad3-G595R* and *SSL1-T242I* mutants display evidence of altered transcription (Table 4) it is possible that this is a response by TFIIF to lesions encountered during transcription of a damaged DNA template. Restoration of wild-type SRR in the *rad3-G595R SSL1-T242I* double mutant suggests that this is a function of the heteropentamer and that the mutations may make compensatory structural changes to the complex. Two-hybrid analysis with wild-type and mutant Rad3 and Ssl1 fusion proteins suggest that *rad3-G595R* and *SSL1-T242I* may alter intersubunit interactions, supporting this hypothesis.

Alternatively, the dominant SRR phenotypes of the *rad3-G595R* and *SSL1-T242I* mutants (Table 5) may indicate that the *rad3-G595R* and *SSL1-T242I* gene products actively inhibit the degradation of the ends of broken DNA molecules by failing to release them and interfering with exonuclease access. The fact that the mutation in *rad3-G595R* alters the putative DNA binding domain (Gorbalya *et al.* 1995) of the helicase supports this hypothesis. Further, the compensatory effects of the *rad3-G595R* and *SSL1-T242I* mutations in the double mutant suggest that Rad3p and Ssl1p together control the access of exonucleases to the DSBs. Interestingly, Garfinkel and colleagues have recently isolated alleles of *RAD3* and *SSL2* that may stimulate Ty transposition by stabilizing Ty cDNA (Lee *et al.* 1998). Together, these analyses indicate that a complex involving several NER and TFIIF-associated proteins influences genome stability by determining the stability of the ends of DNA molecules.

Another possibility is that the SRR phenotypes of the *rad3-G595R* and *SSL1-T242I* mutants may result from defective transcription of genes that encode SRR control factors. Consistent with this suggestion, the *SSL1-T242I* allele suppresses both the gene expression (Table 4) and SRR (Figures 2 and 3; Table 5) phenotypes conferred by *rad3-G595R*. However, the SRR phenotype of the *rad3-G595R* mutant is dominant (Table 5) while its gene expression phenotype is recessive (Table 4), indicating that Rad3p has gained a function that alters

SRR while it has lost an activity required for proper gene expression. This suggests that the relationship between the SRR and transcription control functions of Rad3p may not be at the level of gene expression.

Our analysis of the effects of the *SSL1-T242I* and *SSL1-3* mutations on SRR revealed an unusual pattern of genetic control. The *SSL1-T242I* and *SSL1-3* alleles can suppress their own effect on SRR in homozygous mutant diploid cells and haploid cells that have one chromosomal copy and one centromere-plasmid copy of the *SSL1-T242I* allele (Table 5). One possible explanation for this effect could be that having two copies of these mutant alleles alters *SSL1* expression in a way that nullifies their individual effects on SRR. We found, however, that the suppression is not due to altered transcription of *SSL1* because steady-state levels of *SSL1* mRNA were the same in wild-type, *SSL1-T242I/SSL1* heterozygous, and *SSL1-T242I/SSL1-T242I* homozygous mutant diploid cells (T. Negritto and A. Bailis, unpublished results).

Another possible explanation for the self-suppressing effect of *SSL1-T242I* is suggested by the interactions of the Ssl1-T242I mutant fusion proteins in our two-hybrid experiments. We found that the Ssl1-T242I fusion protein displays twofold and fourfold enhanced ability to interact with wild-type Rad3 and Tfb1 fusion proteins, respectively (Table 6), perhaps indicating that the altered SRR phenotype of the *SSL1-T242I* mutant is a result of changes within the heteropentamer. Our data also indicate a Ssl1-T242I fusion protein interaction stronger by sixfold than interactions of Ssl1 wild-type or Ssl1 wild-type and Ssl1-T242I mutant fusion proteins (Table 6). This indicates that Ssl1-T242Ip mutant subunits may tend to self-associate, which could interfere with the assembly of the heteropentamer if a significant proportion of Ssl1-T242Ip is sequestered. Increasing the copy number of the *SSL1-T242I* allele might lead to the sequestration of a greater proportion of Ssl1-T242Ip, separating it from the complex that brings about altered SRR. Previously, it was shown that an allele of *TFB1* that blocks the interaction between Tfb1p and Ssl1p confers temperature-sensitive growth and UV sensitivity phenotypes (Matsui *et al.* 1995; Sweder *et al.* 1996). Together with our observations this work supports the idea that specific interactions between the subunits of the heteropentamer control its various biological functions, allowing diverse cellular processes to be controlled by a limited set of proteins.

We thank J. Nickoloff, D. Garfinkel, A. Rattray, S. Gangloff, and anonymous reviewers for critiquing the manuscript. We also thank P. Hanawalt, L. Bardwell, A. Lehmann, J. Termini, B. Shen, R.-J. Lin, T. Krontiris, and J. Rossi for helpful discussions. In addition we thank J. McDonald, L. Bardwell, L. Scherer, T. Donahue, H. Klein, S. Elledge, S. Fields, J. Feaver, J. Nickoloff, F. Heffron, and P. Hieter for providing yeast strains and plasmids. This work was supported by U.S. Public Health Service grants GM-57484 and CA-33572 and funds from the Beckman Research Institute and the City of Hope National Medical Center.

LITERATURE CITED

- Bailis, A. M., and S. Maines, 1996 Nucleotide excision repair gene function in short-sequence recombination. *J. Bacteriol.* **173**: 2136–2140.
- Bailis, A. M., and R. Rothstein, 1990 A defect in mismatch repair in *Saccharomyces cerevisiae* stimulates ectopic recombination between homeologous genes by an excision repair dependent process. *Genetics* **126**: 535–547.
- Bailis, A. M., L. Arthur and R. Rothstein, 1992 Genome rearrangement in a *top3* mutant of *Saccharomyces cerevisiae* requires a functional *RAD1* excision repair gene. *Mol. Cell. Biol.* **12**: 4988–4993.
- Bailis, A. M., S. Maines and M. C. Negritto, 1995 The essential helicase gene *RAD3* suppresses short-sequence recombination in *Saccharomyces cerevisiae*. *Mol. Cell. Biol.* **15**: 3998–4008.
- Bardwell, L., A. J. Bardwell, W. J. Feaver, J. Q. Svejstrup, R. D. Kornberg *et al.*, 1994 Yeast *RAD3* protein binds directly to both *SSL2* and *SSL1* proteins: implications for the structure and function of transcription/repair factor b. *Proc. Natl. Acad. Sci. USA* **91**: 3926–3930.
- Britten, R. J., and D. E. Kohne, 1968 Repeated sequences in DNA. *Science* **161**: 529–540.
- Christiansen, T. W., R. S. Sikorski, M. Dante, J. H. Shero and P. Hieter, 1991 Multifunctional yeast high-copy number shuttle vectors. *Gene* **110**: 119–122.
- Cochran, W. G., 1954 Some methods for strengthening the common chi-square tests. *Biometrics* **10**: 417–427.
- Datta, A., A. Adjiri, L. New, G. F. Crouse and S. Jinks-Robertson, 1996 Mitotic crossovers between diverged sequences are regulated by mismatch repair proteins in *Saccharomyces cerevisiae*. *Mol. Cell. Biol.* **16**: 1085–1093.
- de Wind, N., M. Dekker, A. Berns, M. Radman and H. teRiel, 1995 Inactivation of the mouse *MSH2* gene results in mismatch repair deficiency, methylation tolerance, hyperrecombination, and predisposition to cancer. *Cell* **82**: 321–330.
- Elion, E., and J. R. Warner, 1984 The major promoter element of rDNA lies 2-kb upstream. *Cell* **39**: 663–673.
- Feaver, W. J., J. Q. Svejstrup, L. Bardwell, A. J. Bardwell, A. Buratowski *et al.*, 1993 Dual roles of a multiprotein complex from *Saccharomyces cerevisiae* in transcription and DNA repair. *Cell* **75**: 1379–1387.
- Feinstein, S. I., and K. B. Low, 1986 Hyper-recombining recipient strains bacterial conjugation. *Genetics* **113**: 13–33.
- Fields, S., and O. K. Song, 1989 A novel genetic system to detect protein-protein interactions. *Nature* **340**: 1046–1051.
- Fischer, L., M. Gerard, C. Chalut, Y. Lutz, S. Humbert *et al.*, 1992 Cloning of the 62-kilodalton component of basic transcription factor BTF2. *Science* **257**: 1392–1395.
- Friedberg, E. C., W. Siede and A. J. Cooper, 1991 Cellular responses to DNA damage in yeast, pp. 147–192 in *The Molecular and Cellular Biology of the Yeast Saccharomyces: Genome Dynamics, Protein Synthesis and Energetics*, edited by J. R. Broach, J. R. Pringle and E. W. Jones. Cold Spring Harbor Laboratory Press, Cold Spring Harbor, NY.
- Gerard, M., L. Fischer, V. Moncollin, J. M. Chipoulet, P. Chambon *et al.*, 1991 Purification and interaction properties of the human RNA polymerase B(II) general transcription factor BTF2. *J. Biol. Chem.* **266**: 20940–20945.
- Gileadi, O., W. J. Feaver and R. D. Kornberg, 1992 Cloning of a subunit of yeast RNA polymerase II transcription factor b and CTD kinase. *Science* **257**: 1389–1392.
- Gorbalya, A. E., E. V. Koonin, A. P. Donchenko and V. M. Blinov, 1989 Two related superfamilies of putative helicases involved in replication, recombination, repair and expression of DNA and RNA genomes. *Nucleic Acids Res.* **17**: 4713–4730.
- Gu, Y., H. Alder, T. Nakamura, S. A. Schichman, R. Prasad *et al.*, 1994 Sequence analysis of the breakpoint cluster region in the *ALL-1* gene involved in acute leukemia. *Cancer Res.* **54**: 2327–2330.
- Guzder, S. N., H. Qiu, C. H. Sommers, P. Sung, L. Prakash *et al.*, 1994 DNA repair gene *RAD3* of *Saccharomyces cerevisiae* is essential for transcription by RNA polymerase II. *Nature* **367**: 91–94.
- Hinnen, A., J. B. Hicks and G. R. Fink, 1978 Transformation of yeast. *Proc. Natl. Acad. Sci. USA* **75**: 1929–1933.
- Hoejmakers, J. H. J., 1993 Nucleotide excision repair II: from yeast to mammals. *Trends Genet.* **9**: 211–217.
- Hoffman, C. S., and F. Winston, 1987 A ten-minute DNA preparation efficiently releases autonomous plasmids for transformation of *Escherichia coli*. *Gene* **94**: 267–272.
- Humbert, S., H. van Vuuren, Y. Lutz, J. H. J. Hoejmakers, J. M. Egly *et al.*, 1994 p44 and p34 subunits of the BTF2/TFIIH transcription factor have homologies with SSL1, a protein involved in DNA repair. *EMBO J.* **13**: 2393–2398.
- Ito, H., Y. Fukuda, K. Murata and A. Kimura, 1983 Transformation of intact yeast cells treated with alkali cations. *J. Bacteriol.* **153**: 63–168.
- Jinks-Robertson, S., M. Michelitch and S. Ramcharan, 1993 Substrate length requirements for efficient mitotic recombination in *Saccharomyces cerevisiae*. *Mol. Cell. Biol.* **13**: 3937–3950.
- Klein, H. L., 1995 Genetic control of intrachromosomal recombination. *BioEssays* **17**: 147–159.
- Lee, B.-S., C. P. Lichtenstein, B. Faiola, L. A. Rinckel, W. Wysock *et al.*, 1998 Posttranslational inhibition of Ty1 retrotransposition by nucleotide excision repair/transcription factor TFIIF subunits Ssl2p and Rad3p. *Genetics* **148**: 1743–1761.
- Leung, W. Y., A. Malkova and J. E. Haber, 1997 Gene targeting by linear duplex DNA fragments occurs by assimilation of a single strand that is subject to preferential mismatch correction. *Proc. Natl. Acad. Sci. USA* **94**: 6851–6856.
- Maniatis, T., E. F. Fritsch and J. Sambrook, 1989 *Molecular Cloning: A Laboratory Manual*. Cold Spring Harbor Laboratory Press, Cold Spring Harbor, NY.
- Manivaskam, P., S. C. Weber, J. McElver and R. H. Schiestl, 1995 Micro-homology mediated PCR targeting in *Saccharomyces cerevisiae*. *Nucleic Acids Res.* **23**: 2799–2800.
- Matsui, P., J. DePaulo and S. Buratowski, 1995 An interaction between the Tfb1 and Ssl1 subunits of yeast TFIIF correlates with DNA repair activity. *Nucleic Acids Res.* **23**: 767–772.
- Miller, J. H., 1972 *Experiments in Molecular Genetics*. Cold Spring Harbor Laboratory Press, Cold Spring Harbor, NY.
- Montelone, B. A., M. E. Hoekstra and R. E. Malone, 1988 Spontaneous mitotic recombination in yeast: the hyper-recombinational *rem1* mutations are alleles of the *RAD3* gene. *Genetics* **119**: 289–301.
- Naumovski, L., and E. C. Friedberg, 1986 Analysis of the essential and excision repair functions of the *RAD3* gene of *Saccharomyces cerevisiae* by mutagenesis. *Mol. Cell. Biol.* **6**: 1218–1227.
- Negritto, M. T., X. Wu, T. Kuo, S. Chu and A. M. Bailis, 1997 Influence of DNA sequence identity on efficiency of targeted gene replacement. *Mol. Cell. Biol.* **17**: 278–286.
- Nickoloff, J., E. Y. Chen and F. Heffron, 1986 A 24-base pair DNA sequence from the *MAT* locus stimulates intergenic recombination in yeast. *Proc. Natl. Acad. Sci. USA* **83**: 7831–7835.
- Petes, T. D., and C. W. Hill, 1988 Recombination between repeated sequences in microorganisms. *Annu. Rev. Genet.* **22**: 147–168.
- Petit, M.-A., J. Dimpfl, M. Radman and H. Echols, 1991 Control of large chromosomal duplications in *Escherichia coli* by the mismatch repair system. *Genetics* **129**: 327–332.
- Radman, M., 1988 Mismatch repair and genetic recombination, pp. 169–192 in *Genetic recombination*, edited by R. Kucherlapati and G. Smith. American Society for Microbiology, Washington, DC.
- Rayssiguier, C., D. S. Thaler and M. Radman, 1989 The barrier to recombination between *Escherichia coli* and *Salmonella typhimurium* is disrupted in mismatch-repair mutants. *Nature* **342**: 396–401.
- Reynolds, R. J., and E. C. Friedberg, 1981 Molecular mechanisms of pyrimidine dimer excision in *Saccharomyces cerevisiae*: incision of ultraviolet irradiated deoxyribonucleic acid in vivo. *J. Bacteriol.* **146**: 692–704.
- Rothstein, R., 1979 Deletions of a tyrosine tRNA gene in *S. cerevisiae*. *Cell* **17**: 185–190.
- Rothstein, R., 1991 Targeting, disruption, replacement, and allele rescue: integrative DNA transformation in yeast. *Methods Enzymol.* **194**: 281–301.
- Rubnitz, J., and S. Subramani, 1984 The minimum amount of homology required for homologous recombination in mammalian cells. *Mol. Cell. Biol.* **4**: 2253–2258.
- Sancar, A., 1994 Mechanisms of DNA excision repair. *Science* **266**: 1954–1956.
- Schaeffer, L., V. Moncollin, R. Roy, A. Staub, M. Mezzina *et al.*,

- 1994 The *ERCC2* DNA repair gene is associated with the class II BTF2/TFIIH transcription factor. *EMBO J.* **13**: 2388–2392.
- Schichman, S. A., M. A. Caliguri, M. P. Strout, S. L. Carter, Y. Gu *et al.*, 1994 *ALL-1* tandem duplications in acute myeloid leukemia with a normal karyotype involves homologous recombination between Alu elements. *Cancer Res.* **54**: 4277–4280.
- Schneider, J. C., and L. Guarente, 1991 Vectors for expression of cloned genes in yeast: regulation, overproduction and underproduction. *Methods Enzymol.* **194**: 373–388.
- Selva, E. M., L. New, G. F. Crouse and R. S. Lahue, 1995 Mismatch correction acts as a barrier to homeologous recombination in *Saccharomyces cerevisiae*. *Genetics* **139**: 1175–1188.
- Shen, P., and H. V. Huang, 1986 Homologous recombination in *Escherichia coli*: dependence on substrate length and homology. *Genetics* **112**: 441–457.
- Sherman, F., G. R. Fink and J. B. Hicks, 1986 *Methods in Yeast Genetics*. Cold Spring Harbor Laboratory Press, Cold Spring Harbor, NY.
- Sikorski, R. S., and J. D. Boeke, 1991 In vitro mutagenesis and plasmid shuffling: from cloned gene to mutant yeast. *Methods Enzymol.* **194**: 302–318.
- So, C. W., Z. G. Ma, C. M. Price, S. Dong, S. J. Chen *et al.*, 1997 MLL self fusion mediated by Alu repeat homologous recombination and prognosis of AML-M4/M5 subtypes. *Cancer Res.* **57**: 117–122.
- Song, J. M., B. A. Montelone, W. Siede and E. C. Friedberg, 1990 Effects of multiple yeast *rad3* mutant alleles on UV sensitivity, mutability, and mitotic recombination. *J. Bacteriol.* **172**: 6620–6630.
- Sung, P., L. Prakash, S. W. Matson and S. Prakash, 1987 *RAD3* protein of *Saccharomyces cerevisiae* is a DNA helicase. *Proc. Natl. Acad. Sci. USA* **84**: 8951–8955.
- Sung, P., D. Higgins, L. Prakash and S. Prakash, 1988 Mutation of lysine-48 to arginine in the yeast *RAD3* protein abolishes its ATPase and DNA helicase activities but not the ability to bind ATP. *EMBO J.* **7**: 3263–3269.
- Sweder, K. S., R. Chun, T. Mori and P. C. Hanawalt, 1996 DNA repair deficiencies associated with mutations in genes encoding subunits of transcription initiation factor TFIIH in yeast. *Nucleic Acids Res.* **24**: 1540–1546.
- Thomas, B. J., and R. Rothstein, 1989 The genetic control of direct-repeat recombination in *Saccharomyces*: the effect of *rad52* and *rad1* on mitotic recombination of a *GAL10* transcriptionally regulated gene. *Genetics* **123**: 725–738.
- Waldman, A. S., and R. M. Liskay, 1988 Dependence of intrachromosomal recombination in mammalian cells on uninterrupted homology. *Mol. Cell. Biol.* **8**: 5350–5357.
- Wallis, J. W., G. Chrebet, G. Brodsky, M. Rolfe and R. Rothstein, 1989 A hyper-recombination mutation in *S. cerevisiae* identifies a novel eukaryotic topoisomerase. *Cell* **58**: 409–419.
- Wang, Z., J. Q. Svejstrup, W. J. Feaver, X. Wu, R. D. Kornberg *et al.*, 1994 Transcription factor b (TFIIH) is required during nucleotide excision repair in yeast. *Nature* **368**: 74–76.
- Wilcox, D. R., and L. Prakash, 1981 Incision and postincision step of pyrimidine dimer removal in excision-defective mutants of *Saccharomyces cerevisiae*. *J. Bacteriol.* **148**: 618–623.
- Yoon, H., S. P. Miller, E. K. Pabich and T. F. Donahue, 1993 *SSL1*, a suppressor of a *HIS4* 5'-UTR stem-loop mutation, is essential for translation initiation and affects UV resistance in yeast. *Genes Dev.* **6**: 2463–2477.

Communicating editor: M. Lichten